Available online at www.sciencedirect.com
SCIENCE DIRECT®
Chemical Physics Letters 392 (2004) 319–323
CHEMICAL PHYSICS LETTERS
www.elsevier.com/locate/cplett

Gating effect of suspended multiwalled carbon nanotube with all-shell rooted from electrodes: parallel growth from ferromagnetic catalytic contact

Yun-Hi Lee [a,*], Chang-Woo Lee [b], Dong-Ho Kim [b], Yoon-Teak Jang [c], Chang-Hoon Choi [c], Kyung-Sik Shin [c], Byeong-Kwon Ju [c]

[a] *Department of Physics, Korea University, Anam-Dong 5Ga 1, Sungbuk-Gu, Seoul 136-701, Republic of Korea*
[b] *Department of Physics, Yeungnam University, Kyunggsan, Kyungpook 712-749, Republic of Korea*
[c] *Microsystem Center, KIST, Seoul 136-791, Republic of Korea*

Received 12 March 2004; in final form 20 May 2004
Available online 15 June 2004

Abstract

We describe the gate coupling of a rooted grown suspended carbon nanotube (CNT) between two microsized catalytic contact electrodes using a direct parallel growth technique. All-shell Multiwalled carbon nanotubes (MWNTs) were bonded to contact electrodes because MWNTs were grown from the electrodes. The response characteristics of the devices with the gate voltage show typical p-type field effect transistor function at a high-temperature regime and asymmetric Coulomb blockage behavior in low temperatures. Results of the observation suggest that our unique structure, i.e., catalytic ferromagnetic electrode/all-shell bonded MWNT/ferromagnetic electrode, made by direct parallel growth may be a promising key element for nanoelectronics and nano-electro-mechanical-systems (NEMS).
© 2004 Elsevier B.V. All rights reserved.

Multiwalled carbon nanotubes (MWNTs) are among the key materials for nanoelectronics and nanoelectro-mechanical-systems (NEMS). Now, MWNTs are easily obtained in most laboratories, having many types of properties, for which reason they should be studied systematically and utilized more actively. From a practical viewpoint, the concentric multi-shell structure of MWNTs has an intrinsic obstacle useful for its electrical properties. Several research groups have studied the effect of the shell structure in MWNTs on the carrier flow between drain and source electrodes. Based on a low-temperature study of MWNTs by Bachtold et al. [1], it was concluded that in MWNTs side-bonded to metal electrodes, only the outermost shell effectively contributes to electrical transport in a low-bias region. In a high bias regime, the IBM group showed the electronic character and interaction of different shells in MWNTs, indicating the contribution of inner shells by controlled breakdown method [2,3].

Now, it is generally thought that the coupling or interlayer charge transport between the outer shell and an adjacent inner shell is expected to be thermally activated [4]. Recently, a study by the Riken group [5] showed the fact that multiple intertube tunnel junctions formed underneath the electrodes dominated intertube charge transport in an MWNT system. On the other hand, Kanda et al. [6] reported that the contact barrier at M (metal on tube)-MWNT-M critically depends on the electrode material rather than on the detailed shell structures of MWNTs, based on the assumption that MWNTs might have much adsorbed oxygen when they are in a vacuum chamber for the deposition of electrode materials, because no passivation occurred to cause exposure to air. Hence, hard oxidizing electrodes such as Pt do not form a barrier, i.e., oxide, at the interface while Ti could be oxidized easily. Anyway, each of the shells in a MWNT possesses metallic or semiconducting

* Corresponding author. Fax: +8229273292.
E-mail address: yh-lee@korea.ac.kr (Y.-H. Lee).

0009-2614/$ - see front matter © 2004 Elsevier B.V. All rights reserved.
doi:10.1016/j.cplett.2004.05.076

properties according to its chirality, in principle, and furthermore, each shell also interacts with adjacent shells.

In the case of suspended nanotubes, last year the Dai and colleagues [7] showed very high-gain ambipolar transistor function for a suspended carbon nanotube (CNT) bridge which formed by the thermal chemical vapor deposition (CVD) method using Mo electrodes, with basement of poly-Si at very high temperature. On the other hand, Nygard and Cobden [8] presented a suspended CNT technique which uses a self-aligned oxide etch to suspend individual SWNT between metallic electrodes and observed the effect of a quantum island, i.e., single electron tunneling, in suspended CNTs.

In this work, we have studied the gate function of the suspended all-shell MWNTs bonded to electrodes. As reported in our previous works [9,10], we introduced a method to form suspended MWNTs, which were bridged between the pre-patterned catalytic contact electrodes and furthermore, can be measured electrically without any post-processing after synthesis of MWNTs. A Nb or SiO_2 layer on top of the catalytic metal was deposited to control the parallel growth of CNT between two ferromagnetic catalytic electrodes and to passivate ferromagnetic contact metals (Ni, Co, etc.) after the growth. As a result, CNTs by low-temperature rapid thermal CVD process are found to grow from one catalytic ferromagnetic electrode to another electrode without additional post-lithographic processes. In our experiment, the layer structure was prepared by stacking Nab-catalyst (Co)–SiO_2 on a heavily-doped Si substrate. The samples were examined by field emission scanning electron microscope (Hitachi S4300). Fig. 1 shows the typical SEM image of the laterally grown CNT bridges between two catalytic pads. The CNTs grown under this condition are very straight, with little bending across the whole length. The diameter of these selectively grown MWNTs is about 10–30 nm within the resolution limit of the SEM image, and the number of walls are about 5 by HRTEM measurement. After optimizing junction, we investigated the field and temperature effect of the operating characteristics of 3 terminal devices with the back gate electrode to check both the field effect transistor function and possible controllability of the promising structure of integrated CNT logic gates. For more than 30 devices measured in this work, 40% of the tested devices showed a semiconducting behavior with change of current under gate biasing, although the degree of the gating effect is different depending on the specific sample. The resistance of our suspended MWNTs range from ∼200 kΩ to ∼20 MΩ. The electrical characteristics, source-drain current (I_D) versus source-drain voltage (V_{SD}), as a function of the gate voltages V_G for the typical 3-terminal CNT devices are shown in Fig. 2a,b. As can be seen in Fig. 2a which was collected under a vacuum of 10^{-6} Torr, the device approximates a voltage variable resistor reasonably good for small values of both positive and negative V_{SD} of $-400 \sim +400$ mV with a 2-terminal resistance of $R = 10$ MΩ at $V_G = 0$ V. The dynamic range of the linear variable resistance region is relatively wider in our devices compared to conventional metal-oxide-semi-

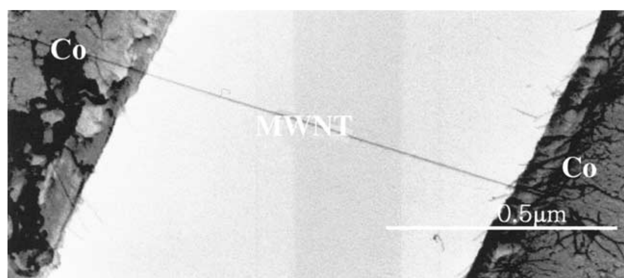

Fig. 1. A typical SEM image of the all-shell multiwalled carbon nanotube (MWNT) rooted from ferromagnetic contact electrodes (Co).

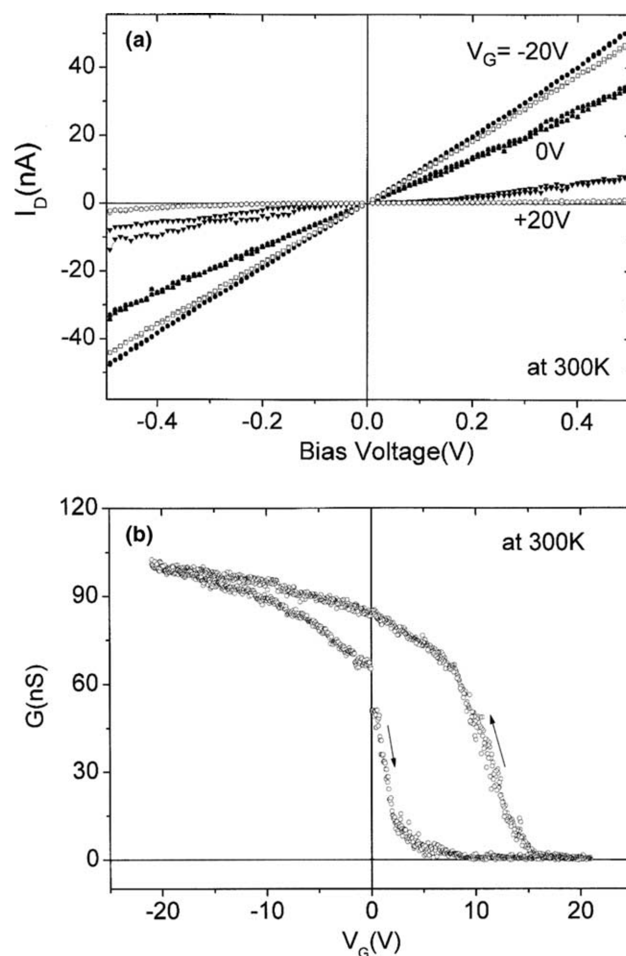

Fig. 2. (a) Current–voltage characteristics of the MWNT junctions and (b) their transfer characteristics of all-shell MWNT rooted from Co electrodes.

conductor field-effect transistor (MOSFET). As is well known already, the role of the V_G is to change the value of R_{CNT} through Fermi level (E_F) modulation, thus changing the slope. Fig. 2a shows that positive gate bias reduces the current, while negative V_G increases the current, thus the device behaves as a *p*-channel FET similar to other systems such as an individual SWNT [11,12].

The conductance (G) modulation of the directly bridged CNW is about 3–4 orders of magnitude as shown in the inset at a low V_G regime, and G (i.e., $1/R$) shows linear increase as a function of $|V_G - V_T|$. In general, complete saturation of the drain current for values of V_{SD} greater than the pinch-off voltage will only be observed in FETs with very large channel lengths. As the drain-to-source spacing of FET is reduced, like in our case, to a scale of below 1 μm, the saturation properties of the I_D deteriorate normally. Other mechanisms can contribute to the degradation of the I_D, but they are beyond the scope of this work. Adapting the procedure given by Martel and colleagues, the hole density and mobility at room temperature for the p-type FET with ferromagnetic catalytic electrodes can be determined if we assume a homogeneous hole distribution along the CNT and the total charge Q on the nanotube as $Q = CV_T$, where C is the device capacitance. If we model the nanotube as a metallic cylinder, the device capacitance per unit length with respect to the back gate is $C/L \approx 2\pi\varepsilon\varepsilon_0/\ln(L/d)$, with d and L being the carbon nanotube radius and length, and ϵ and h the average dielectric constant and the thickness of the device. Using $L = 1000$ nm, $d = 30$ nm, $h = 1000$ nm, and $\varepsilon \approx 2.5$ provides a 1-dimensional hole density of $p = Q/eL \approx 4.7 \times 10^6$ cm^{-1} from $V_T = 6$ V. Assuming diffusive transport in our CNT at room temperature similar to the SWNT bundles, we can estimate the hole mobility from the transconductance, g_m, of the CNT FET. As previously described, since the carrier mobility is constant in the linear regime of I_D–V_{SD} curve, we obtain $g_m = \partial I_D/\partial V_G = \mu_h (C/L)^2 V_{SD} = 0.14$ nA/V, 2.88 nA/V at $V_{SD} = 10$ and 100 mV, respectively, corresponding to a hole mobility of $\mu_h \approx 11$ and 230 cm^2/V s. Although this mobility value is very low compared to that of the SWNT–FET with Mo containing electrodes by Dai and colleagues [7], the mobility as well as the transconductance indicates that the holes within nanotubes contain a fewer number of scattering centers. On the other hand, for temperature dependence of g_m at $V_{SD} = 100$ mV, we observed $g_m = 2.88$, 1.15, and 0.30 nA/V at 300, 250, and 150 K, respectively, and this temperature dependence should come from mobility. Here, if we assume that the conductance of this junction is limited by scattering within the MWNT, the mobility can be derived by taking a linear approximation of $G(V_g)$. The mobility μ_h can be related to the 1-dimensional diffusion coefficient $D = \upsilon_F l$, and $D = \mu E_F/e$ where $E_F \approx 0.5$ eV is the Fermi energy, $\upsilon_F \approx 10^6$ m s^{-1} is the Fermi velocity, and l the scattering mean free path. From this correlation, we obtained$D \approx 0.15$ m^2 s^{-1} and $l \approx 15$ nm. Of course, these values are the lower limits for μ, D, and l, as indicated by the Schonenberger group, because there are other contributions such as contacts and impurities, etc. [12,13].

Using the device structure, we repeated measurements to examine the gating effect at low-temperature regimes. At $T = 2$ K we obtained current characteristics as a function of drain-to-source bias and gate voltage. A typical example of the current–voltage and the corresponding differential conductance characteristics measured at $T = 2$ K on a junction with an individual CNT bridge. These measurements clearly demonstrate gap-like features. The differential conductance dI/dV vs gate voltage V_G exhibits Coulomb blockade (CB) diamonds, implying that quantum islands are formed in the CNT junction at low-temperature regimes.

In order to examine more systematically the Coulomb blockade structure in the junction, we constructed surface and grayscale plots from I–V_{SD} curves at different V_G bias values, as shown in Fig. 3a,b, respectively. The rhombus shapes of the current suppressed regions and the V_G induced modulation are clearly visible, indicating the existence of quantum islands. Assuming the gaps due to the density of states and due to Coulomb blockades both affect I–V characteristics, we can relate the slope of the constant current curves to the ratio C_g/C_{source} and C_g/C_{drain} [14]. Using the slopes shown in Fig. 3c measured at 2 K and $\Delta V_G \approx 20$ mV, we obtain $C_G = 29$ aF, $C_{left} = 23$ aF and $C_{right} = 18$ aF for the capacitances between the dots and the left/right (source/drain) electrode. So the total capacitance of the system C_Σ is 70 aF, which yields a charging energy U of 20 meV. Here, C_Σ is the total capacitance corresponding to the islands in the CNT junction.

On the other hand, we derived the coupling factor α which measures the effectiveness of the coupling capacitance between the CNT bridge and the gate, i.e. $\alpha = C_g/C_\Sigma = U_c/\Delta V_g$. Here, ΔV_g is the single-electron period in gate voltage. We found $\alpha \approx 0.41$ for the direct, lateral grown CNT junction with two catalytic ferromagnetic contact electrodes. This value is the highest reported so far for a CNT junction with back gate electrode.

Next, we estimated the geometrical capacitance and compared that with the observed value. The estimated total capacitance $C_{geometry} = 2\pi L\varepsilon_r\varepsilon_0/\ln[2L/d]$ is about 25 aF, corresponding to the bridge length and diameter of a nanotube of about 1 μm and 20 nm. After we compared this with the experimental value of 70 aF, we noticed a difference factor of two. We interpreted this to be an indication that the actual junction size was shorter than the geometrical lengths confirmed in the SEM measurements. A possible explanation for this

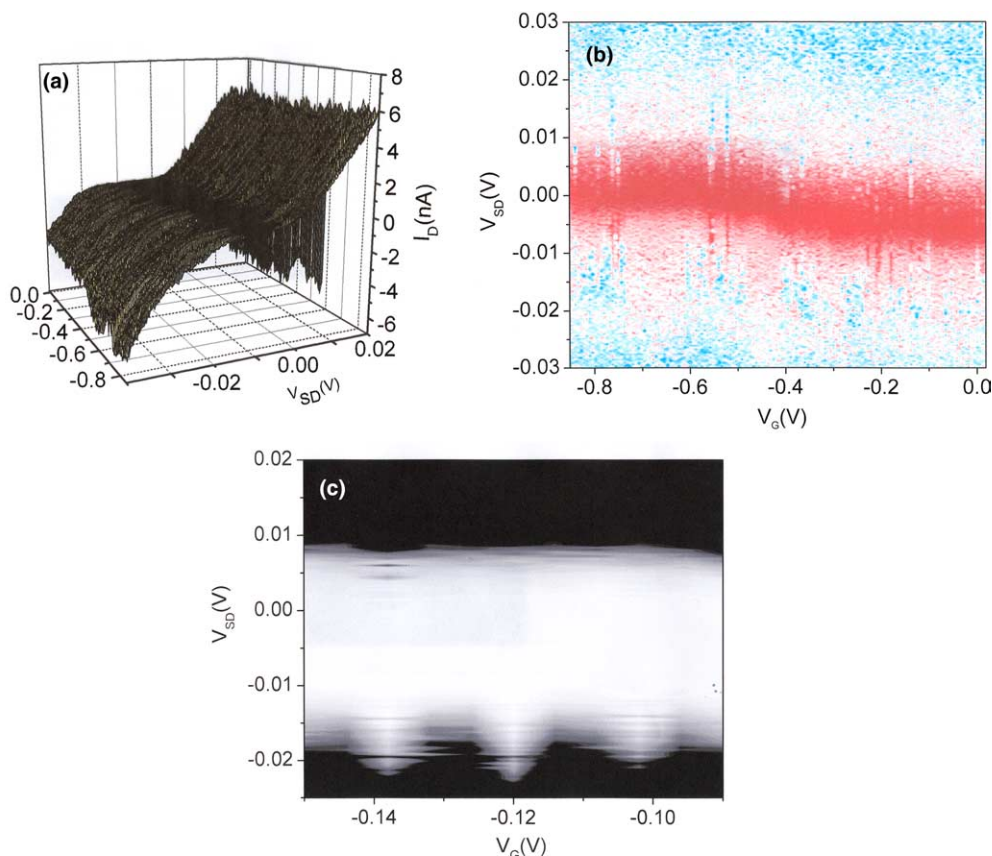

Fig. 3. (a) Gate voltage dependence of I–V_{SD} curves at 2 K, (b) grayscale plots obtained from $dI/dV - V_{SD} - Vg$ values over the full measured range and (c) extended view of CB diamonds in a limited V_G regime.

shortening is the smearing of the contact electrodes onto the CNT bridge during the period when CNT was growing from the contact electrodes, which also functioned as a catalytic material for growing CNTs in our work. However, we cannot determine how long the contact electrode and the CNT bridge are.

The presence of the staircase in the experimental $I(V)$ measurements can be explained by the orthodox theory. The $I(V)$ characteristics of nearly symmetrical junctions feature a smooth curve with a Coulomb gap of around zero bas of e/C_{Σ}. In contrast, for strong asymmetric junctions($C_{left} \gg C_{right}$ and $R_{right} \gg R_{left}$) in addition to the Coulomb gap, the $I(V)$ curve shows periodic oscillations with a period $\Delta V_{staircase} = e/C_{right}$. This asymmetricity reappears in Fig. 3c. That is, most of the Coulomb diamonds are asymmetric and distorted as shown in Fig. 3b over the entire measured range. Considering the fact that the slopes of the diamonds correspond to the source-gate capacitance ratio, we found that the CNT bridge has asymmetric couplings to the source and drain electronically. Assuming that our CNT bridge was grown from one of the catalytic contact metals and to opposite catalytic metal electrodes, we understood the electronic asymmetricity of the contacts.

In conclusion, FET and SET functions were observed for parallel grown all-shell MWNT bonded to contact electrodes. As compared to end-, top-, and side contacts, asymmetry of the contact properties of our MWNTs is very much higher. We assume that the asymmetry might be related to growth of CNT from one side of the contact electrode to the opposite side of the electrodes. However, a more systematic study such as in situ TEM on both junction areas will be required.

Acknowledgements

We acknowledge all of members of DIANA at KIST for their sincere support. This work was supported by the National R&D Project for NanoCore Technology of the Ministry of Science and Technology in Korea and partly by IMT 2000 and ITRC program.

References

[1] A. Bachtold, C. Strunk, J.P. Salvetat, J.M. Bonard, L. Forró, T. Nussbaumer, C. Schönenberger, Nature (London) 397 (1999) 673.
[2] P.G. Collins, M.S. Arnold, Ph. Avouris, Science 292 (2001) 706.
[3] P.G. Collins, M. Hersam, M. Arnold, R. Martel, Ph. Avouris, Phys. Rev. Lett. 86 (2001) 3128.

[4] P. Avouris, Chem. Phys. 281 (2002) 429.
[5] E. Watanabe, K. Tsukagoshi, D. Kanai, I. Yagi, Y. Aoyagi, Appl. Phys. Lett. 83 (2003) 1429.
[6] A. Kanda, Y. Ootuka, K. Tsukagoghi, Y. Aoyagi, Appl. Phys. Lett. 79 (2001) 1354.
[7] N.R. Franklin, Q. Wang, T.W. Tombler, A. Javey, M.S. Shim, H. Dai, Appl. Phys. Lett. 81 (2002) 913.
[8] J. Nygard, D.H. Cobden, Appl. Phys. Lett. 79 (2001) 4216.
[9] Y.H. Lee, Y.T. Jang, D.H. Kim, J.H. Ahn, B.K. Ju, Adv. Mater 13 (2001) 1371.
[10] Y.H. Lee, Y.T. Jang, C.H. Choi, D.H. Kim, C.W. Lee, B.K. Ju, E.K. Kim, S.S. Yoon, J. Appl. Phys. 91 (2002) 6044.
[11] S.J. Tans, A.R.M. Verschueren, C. Dekker, Nature 393 (1998) 49.
[12] C. Schönenberger, A. Bachtold, C. Strunk, J.-P. Salvetat, L. Ferró, Appl. Phys. A 69 (1999) 283.
[13] B. Babic, M. Iqbal, C. Schönenberger, Nanotechnology 14 (2003) 327.
[14] D.K. Ferry, S.M. Goodnick, in: H. Ahmed, M. Pepper, A. Broers (Eds.), Transport in Nanostructures, Cambridge University Press, Cambridge, UK, 1997.